

KP Cyg: an Unusual Metal-rich RR Lyr Type Star of Long Period

S.M. Andrievsky¹ and V.V. Kovtyukh

*Department of Astronomy and Astronomical Observatory, Odessa National University,
T.G. Shevchenko Park, 65014, Odessa, Ukraine*

scan@deneb1.odessa.ua, val@deneb1.odessa.ua

George Wallerstein

Department of Astronomy, University of Washington, Seattle, WA 98195

wall@astro.washington.edu

S.A. Korotin

*Department of Astronomy and Astronomical Observatory, Odessa National University,
T.G. Shevchenko Park, 65014, Odessa, Ukraine*

serkor@skyline.od.ua

Wenjin Huang

Department of Astronomy, University of Washington, Seattle, WA 98195

hwenjin@astro.washington.edu

ABSTRACT

We present the results of a detailed spectroscopic study of the long period ($P = 0.856$ days) RR Lyrae star, KP Cyg. We derived abundances of many chemical elements including the light species, iron-group elements and elements of the s-processes. Most RR Lyrae stars with periods longer than 0.7 days are metal-deficient objects. Surprisingly, our results show that KP Cyg is very metal rich ($[\text{Fe}/\text{H}] = +0.18 \pm 0.23$). By comparison with a number of short period ($P = 1 \sim 6$ days), metal-rich CWB stars, we suggest that KP Cyg may be a very short period CWB star (BL Her star) rather than an RR Lyrae star. As seen in some CWB stars, KP Cyg shows strong excesses of carbon and nitrogen in its atmosphere. This indicates that the surface of KP Cyg has been polluted by material that has undergone helium burning (to enhance carbon) and proton capture (to transform carbon into nitrogen). We also note that UY CrB, whose

period is 0.929 days, also shows an enhancement of C and N, and that two carbon cepheids of short period, V553 Cen and RT TrA, show similar excesses of carbon and nitrogen.

Subject headings: stars: RR Lyr type, individual: KP Cyg

1. Introduction

The RR Lyrae stars have been known for a long time to be an old population with diverse metallicity (from near solar to $[\text{Fe}/\text{H}] \sim -2.5$). They are present in most globular clusters but in widely different numbers ranging from zero to about 200 (Clement et al. 2001). The general properties of RR Lyrae stars can be found in detail in the book by Smith (1995). Most RR Lyrae stars in the field and in clusters are readily divided into two major categories: the RRc-type with periods from approximately 0.20 d to 0.45 d, and the RRab type with periods from about 0.4 to 1.0 days. There is a statistical correlation between metallicities and periods of RR Lyrae stars that the stars with longer periods are generally more metal-poor.

Very few RR Lyrae stars are known with periods longer than 0.75 days. In his classic paper on the metallicity of RR Lyrae stars Preston (1959) included a few long period stars that he found to be relatively metal-rich. However he subsequently noted that the data of some of those stars, mostly their periods, were in error. Among the recently discovered RR Lyrae stars in the Northern Sky Variability Survey (NSVS), Kinemuchi et al. (2009) have found 21 variables with periods between 0.74 and 0.86 days whose metallicities range from $[\text{Fe}/\text{H}] = -1.50$ to -2.15 dex, similar to the RR Lyrae stars with periods of 0.60 to 0.75 days.

The general picture of the long-period RR Lyrae stars having low metallicity has not been strongly challenged until the discovery of some long-period RR Lyrae stars in the two globulars, NGC 6388 and 6441 (Pritzl et al. 2000). These two massive clusters have unusual color-magnitude diagrams. Their red giant branches are relatively faint indicating that they are relatively metal-rich for globular clusters. A spectroscopic analysis of red giants in NGC 6388 showed that $[\text{Fe}/\text{H}] = -0.7$ (Wallerstein, Kovtyukh, and Andrievsky 2007). For NGC 6441, Gratton et al. (2007) found a metallicity of $[\text{Fe}/\text{H}] = -0.34$. In addition, for NGC 6441, Clementini et al. (2005) found a metallicity of -0.7 from a sample of its RR Lyrae stars. Both horizontal branches consist of a well populated red clump accompanied by a significant number of blue stars including a blue tail in NGC 6441. From Preston's correlation of period and metallicity such high metallicities indicate that the RR Lyrae stars should have short

periods. However Pritzl et al. found a wide range of periods in these clusters including numerous variables with periods larger than 0.75 days.

In an attempt to find field RR Lyrae stars that are similar to those with long periods in NGC 6388 and 6441, we have observed a few RR Lyraes with periods greater than 0.75 days. Among them, KP Cyg appears to be the most unusual. First noted by Vogt (1970) and subsequently confirmed by others (Loomis et al. 1988, Schmidt 2002), KP Cyg has a period of about 0.856 days, quite long for an RR Lyrae star. Preston (1959) found its ΔS value to be around 0, implying that KP Cyg is a metal-rich object. Other than this information, we know little about the star. In this paper we present the results of an analysis of the chemical composition in this star’s atmosphere.

2. Observation and Data Reduction

Spectra of KP Cyg were obtained using the echelle spectrograph on the 3.5-m telescope, at the Apache Point Observatory (APO). The usable wavelength coverage, limited by the red-sensitive 2048×2048 CCD chip, runs from 4000 \AA to 9000 \AA . The resolving power is about 35000. The integration time of each exposure was set to 20~30 minutes to reach good S/N ratios, and to avoid heavy contamination from cosmic ray events. We then combined the spectra that were taken sequentially within one hour, and measured the S/N ratio at the continuum level per pixel in the very clean region between 7550 and 7600 \AA of the combined spectra.

Table 1 lists the dates (JD), phases, the heliocentric radial velocities (V_r), the derived values of T_{eff} and $\log g$ for each phase, and signal-to-noise ratio of each spectrum. Our V_r measurements confirm that the period of KP Cyg is around 0.9 days. We also note the presence of anomalous structures in $H\alpha$ such as line doubling and emission. A comparison of the abundances derived from the spectra having anomalous $H\alpha$ profiles with those derived from the spectra showing normal $H\alpha$ profiles demonstrates that there is no very significant difference among the derived $[\text{Fe}/\text{H}]$ values. We suspect that the anomalous features in the $H\alpha$ line profile originate from the layers far above the line forming region that is relevant to our abundance analysis.

The spectra were extracted from the raw frames using standard IRAF¹ procedures. The continuum level placement, wavelength calibration and equivalent widths measurements were performed with DECH20 code (Galazutdinov 1992). The final equivalent width measure-

¹<http://iraf.noao.edu>

ments are presented in Table A1, whose full content is available only in the electronic edition. A small portion of the table is given here to illustrate its format and content. The equivalent widths of some very strong or seriously blended lines were not measured. Instead, for these lines, we compared their NLTE synthesized profiles directly with the observed spectra in the abundance analysis (see §3.2).

3. Method of Analysis

3.1. Atmospheric Parameters and LTE Elemental Abundances

The LTE elemental abundances were derived using the Kurucz’s WIDTH9 (Kurucz 1996) code with the model atmospheres interpolated from the ATLAS9 model grid. We used $\log gf$ values derived from an inverted solar analysis (Kovtyukh & Andrievsky 1999).

The atmospheric parameters of KP Cyg (T_{eff} , $\log g$, V_t) were determined by meeting a few requirements in our spectroscopic analysis: T_{eff} and V_t were constrained by minimizing the dependence of the derived iron abundance from each Fe I line on their excitation potentials and equivalent widths; $\log g$ was determined by requiring an ionization equilibrium between Fe I and Fe II. While $\log g$ may be calculated using the known luminosities and masses of RR Lyrae stars, we preferred to use the method based on the FeI/FeII ionization equilibrium because the acceleration of the atmosphere during its pulsation cycle is then automatically taken into account.

3.2. NLTE Elemental Abundances

The NLTE effects were considered in deriving the abundances of such elements as carbon, nitrogen, oxygen, sodium, magnesium, aluminum, sulfur, potassium, strontium, and barium. The details of the atomic models used for calculating the NLTE line profiles are described in

Table 1:: Observations of KP Cyg and its atmospheric parameters

Date	JD 2450000+	phase	S/N	V_r (km s ⁻¹)	$T_{\text{eff,K}}$	$\log g$	V_t (km s ⁻¹)	Remarks
2005-11-13	3687.606	.135	46	8.6	7050	2.6	2.5	
2006-11-05	4044.672	.299	47	13.1	6600	3.0	3.3	
2007-05-01	4221.963	.430	73	20.3	6450	3.4	3.5	H α emission
2005-09-24	3637.607	.720	88	35.6	6300	2.4	3.2	H α emission
2006-10-03	4011.720	.800	47	27.5	6650	3.0	4.2	H α emission
2005-09-13	3626.711	.991	91	-1.8	7400	3.0	2.5	

a series of papers by Andrievsky et al. (2001, 2007, 2008, 2009, 2010a,b) for carbon, sodium, aluminum, barium, magnesium, potassium, and strontium respectively, Korotin (2009) — for sulfur, Mishenina et al. (2000) — for oxygen, Lyubimkov et al. (2010) — for nitrogen. The NLTE abundances of these elements were derived using a NLTE spectrum synthesis code adapted from MULTI (see Carlsson (1986) and Korotin et al. (1999a,b)). The list of the lines used in the NLTE calculations and their parameters are given in Table 2.

Because some of the NLTE-treated lines are blended with other lines, we used the combined NLTE and LTE synthetic spectra when we compared the NLTE line profiles with the observed spectra. This was done using the code SYNTHV (Tsymbal 1996), which was developed for LTE spectrum synthesis. We calculated the synthetic spectra for the selected regions comprising the lines of interest and all nearby lines that are found in VALData-base (Kupka et al. 2000). Meanwhile, for each line treated in NLTE, the corresponding b -factors (the ratios of the NLTE to LTE populations in the involved energy levels) were calculated by MULTI and then fed into SYNTHV for calculating the NLTE line source functions. Some examples of the NLTE profile fitting in KP Cyg spectra are shown in Fig. 1.

Our results of the NLTE abundance analysis of KP Cyg need to be compared to the sun. Hence we chose to use the same source for the model atmospheres for both the Sun and KP Cyg. We used the Kurucz’s solar model to derive our NLTE abundances in the Sun in the same way as we did for KP Cyg. Solar equivalent widths were obtained from observations of the asteroid, Vesta, obtained by Don York, using the same instrument (the APO echelle spectrograph) as was used for the KP Cyg spectra. The derived NLTE abundances of the Sun (based on the line list of Table 2) are given in the last column of Table 2.

In Table 3, we show the sensitivity of the NLTE oxygen abundance to the variation of the adopted atmospheric parameters. As one can see, the changes of the parameters within our observational uncertainty ($\Delta T_{\text{eff}} \approx \pm 150\text{K}$, $\Delta \log g \approx \pm 0.2$, and $\Delta V_t \approx \pm 0.3 \text{ km s}^{-1}$) cause only small fluctuations in the derived oxygen abundance ($< 0.2 \text{ dex}$).

4. Discussion

The final derived elemental abundances are given in Table 4. The abundances of the iron-group elements in KP Cyg are consistent with the results by Preston (1959) ($\Delta S = 0$). According to the combined data presented by Smith (1995, Fig. 3.9), there are no RR Lyr stars in globular clusters both with metallicity higher than -1.0 and periods larger than 0.8 days except for a few stars in the two puzzling clusters, NGC 6388 and 6441, and a single star in 47 Tuc. The super-solar metallicity and unusually long period makes KP Cyg even

Table 2:: List of the lines used for NLTE calculations

Ion	λ	χ (eV)	$\log gf$	$\log \epsilon(\text{El})_{\odot}$	Ion	λ	χ (eV)	$\log gf$	$\log \epsilon(\text{El})_{\odot}$		
Cl	5052.17	7.685	-1.30	8.43	NaI	4982.81	2.104	-0.96	6.25		
	5380.34	7.685	-1.62			4982.81	2.104	-1.91			
	6014.83	8.643	-1.58			5682.63	2.102	-0.70			
	6413.55	8.771	-2.00			5688.19	2.104	-1.39			
	6587.61	8.537	-1.13			5688.20	2.104	-0.46			
	6655.51	8.537	-1.79			6154.22	2.102	-1.53			
	7087.83	8.647	-1.44			6160.74	2.104	-1.23			
	7100.12	8.643	-1.47			8183.25	2.102	0.26			
	7108.93	8.640	-1.59			8194.79	2.104	-0.44			
	7111.47	8.640	-1.09			8194.82	2.104	0.51			
	7113.17	8.647	-0.77		MgI	4167.27	4.346	-0.77	7.58		
	7115.17	8.643	-0.93			4702.99	4.346	-0.52			
	7115.18	8.640	-1.47			5172.68	2.712	-0.38			
	7116.99	8.647	-0.91			5183.60	2.717	-0.16			
	7119.65	8.643	-1.15			5528.40	4.346	-0.62			
	7473.30	8.771	-2.04			5711.09	4.346	-1.72			
	7476.17	8.771	-1.57			AlI	6696.02	3.143		-1.48	6.43
	7483.44	8.771	-1.37				6698.66	3.143		-1.78	
	7848.24	8.848	-1.73				7835.30	4.022		-0.64	
	7852.86	8.851	-1.68				7836.13	4.022		-1.64	
7860.88	8.851	-1.15	7836.13	4.022	-0.45						
8335.14	7.685	-0.44	8772.87	4.022	-0.24						
Ni	7442.29	10.330	-0.39	7.89	8773.90		4.022	-0.02	7.16		
	7468.31	10.336	-0.19		8773.90		4.022	-1.32			
	8184.86	10.330	-0.28		Si		6538.60	8.046		-0.93	
	8188.01	10.326	-0.29				6743.44	7.866		-1.20	
	8210.71	10.330	-0.73			6743.53	7.866	-0.85			
	8216.33	10.336	0.09			6743.64	7.866	-0.95			
	8223.12	10.330	-0.32			6748.57	7.868	-1.32			
	8242.38	10.336	-0.32			6748.68	7.868	-0.73			
	8680.28	10.336	0.35			6748.84	7.868	-0.53			
	8683.40	10.330	0.09			6756.85	7.870	-1.67			
	8686.14	10.326	-0.30			6757.01	7.870	-0.83			
	8703.24	10.326	-0.32			6757.17	7.870	-0.24			
	8711.70	10.330	-0.23			8693.93	7.870	-0.51			
	8718.83	10.336	-0.33			8694.63	7.870	0.08			

Table 2:: List of the lines used for NLTE calculations (continued)

Ion	λ	χ (eV)	$\log gf$	$\log \epsilon(\text{El})_{\odot}$	Ion	λ	χ (eV)	$\log gf$	$\log \epsilon(\text{El})_{\odot}$
OI	5577.34	1.967	-8.24	8.71	KI	7664.91	0.000	0.13	5.11
	6155.97	10.740	-0.67			7698.97	0.000	-0.17	
	6156.76	10.741	-0.45		SrII	4077.71	0.000	0.15	2.92
	6158.17	10.741	-0.31			4161.79	2.940	-0.41	
	6300.30	0.000	-9.75			4215.52	0.000	-0.18	
	6363.77	0.020	-10.30		BaII	4554.03	0.000	0.08	2.17
	7771.94	9.146	0.33			4554.05	0.000	-0.79	
	7774.16	9.146	0.19			4554.00	0.000	-1.01	
	7775.38	9.146	-0.03			5853.68	0.604	-1.00	
	8446.24	9.521	-0.52			6141.71	0.704	-0.08	
	8446.35	9.521	0.18			6496.89	0.604	-0.46	
8446.75	9.521	-0.05		6496.89		0.604	-1.32		
				6496.90		0.604	-1.55		

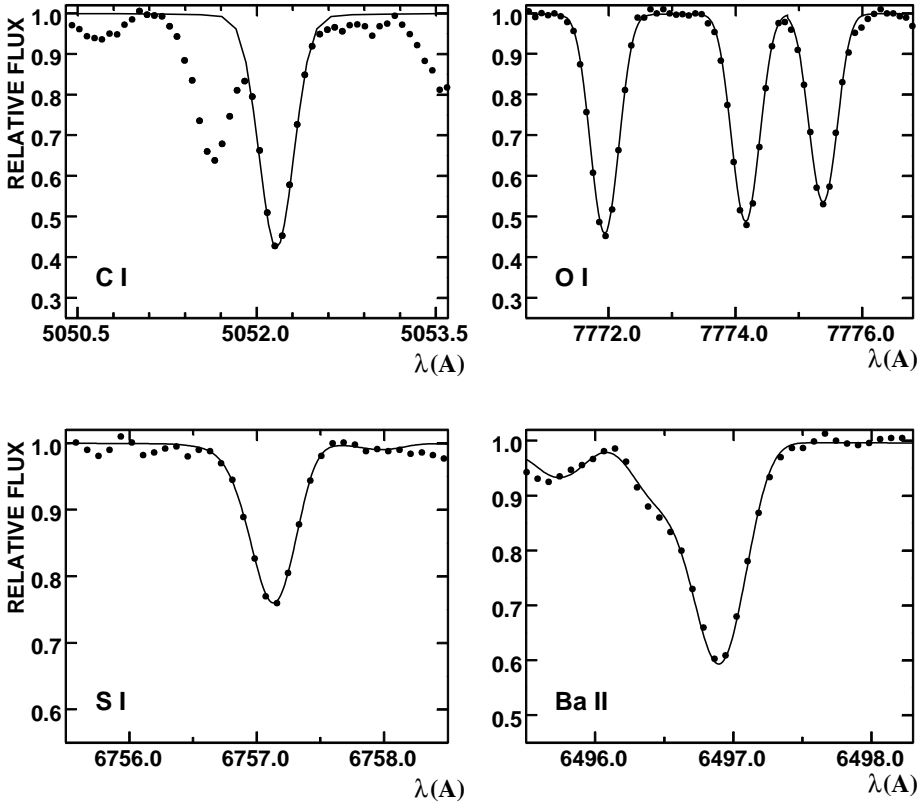


Fig. 1.—: Examples of the best-fit synthesized NLTE profiles (*solid lines*) are over-plotted on the observed spectra (*filled dots*).

Table 3:: Parameter variation and NLTE oxygen abundance for KP Cyg

T_{eff}	$\log g$	V_t	$\log \epsilon(\text{O})$
6600	3.0	3.3	9.05
6450	3.0	3.3	9.15
6750	3.0	3.3	8.96
6600	3.2	3.3	9.15
6600	2.8	3.3	8.98
6600	3.0	3.6	8.96
6600	3.0	3.0	9.14

Table 4:: Elemental abundances in KP Cyg

Ion	$\phi = 0.135$			$\phi = 0.299$			$\phi = 0.430$			$\phi = 0.720$		
	[El/H]	σ	N	[El/H]	σ	N	[El/H]	σ	N	[El/H]	σ	N
Cl*	+0.86	0.13	23	+0.92	0.13	18	+0.95	0.11	19	+0.77	0.15	17
NI*	+0.91	0.14	13	+1.18	0.14	11	+1.32	0.10	11	+0.91	0.15	6
OI*	+0.41	0.12	4	+0.29	0.12	6	+0.34	0.12	6	+0.24	0.12	3
NaI*	+0.54	0.12	6	+0.45	0.12	5	+0.48	0.10	6	+0.50	0.10	6
MgI*	+0.14	0.12	6	-0.05	0.12	3	+0.07	0.10	5	-0.05	0.12	5
AlI*	+0.47	0.17	2	+0.37	0.13	3	+0.44	0.15	6	+0.42	0.15	4
SiI	+0.16	0.12	10	+0.32	0.06	14	+0.29	0.10	17	+0.14	0.18	7
SiII	+0.11	-	1	-	-	-	+0.25	-	2	+0.12	-	2
SI*	+0.26	0.13	5	+0.32	0.13	4	+0.34	0.11	6	+0.21	0.12	2
KI*	+0.27	0.12	1	-0.20	0.12	1	-	-	-	-0.10	0.12	1
CaI	+0.04	0.19	9	+0.03	0.12	9	+0.03	0.15	8	+0.19	0.23	8
ScII	-0.11	0.07	4	+0.32	0.17	6	+0.37	0.16	5	-0.07	0.18	5
TiI	-0.20	-	2	+0.15	0.12	4	+0.11	0.13	6	+0.08	0.20	3
TiII	-0.20	0.04	3	+0.13	0.12	5	+0.14	0.14	5	-0.08	0.16	3
VII	+0.04	-	2	+0.21	-	1	+0.42	0.10	3	+0.36	-	1
CrI	-0.07	0.07	3	+0.09	0.14	4	+0.02	0.12	6	-0.15	0.19	3
CrII	-0.05	0.08	5	+0.17	0.08	5	+0.14	0.11	3	-0.04	0.18	4
MnI	+0.11	-	2	+0.15	0.05	2	+0.16	0.19	3	+0.34	-	2
FeI	+0.09	0.12	68	+0.29	0.10	72	+0.30	0.15	88	+0.05	0.19	59
FeII	+0.09	0.13	17	+0.29	0.08	15	+0.31	0.12	18	+0.08	0.19	10
NiI	+0.06	0.13	15	+0.36	0.13	23	+0.16	0.08	25	+0.16	0.15	12
SrII*	-	-	-	-	-	-	+0.12	0.17	2	-	-	-
YII	+0.08	0.21	3	+0.35	0.16	4	+0.25	0.15	5	+0.08	-	2
BaII*	+0.20	0.14	4	-0.15	0.10	4	-0.20	0.10	4	-0.35	0.10	3
NdII	-	-	-	+0.12	0.02	2	+0.24	0.20	3	+0.25	-	2

Table 4:: Elemental abundances in KP Cyg (continued)

Ion	$\phi = 0.800$			$\phi = 0.991$			Mean [El/H]
	6650/3.0/4.2			7400/3.0/2.5			
	[El/H]	σ	N	[El/H]	σ	N	
Cl*	+0.79	0.15	14	+0.67	0.12	16	+0.83
NI*	+1.14	0.15	9	+1.09	0.12	8	+1.10
OI*	+0.29	0.12	4	+0.34	0.14	4	+0.32
NaI*	+0.51	0.12	5	+0.38	0.14	4	+0.48
MgI*	-0.13	0.12	6	-0.13	0.15	4	-0.02
AlI*	+0.68	–	1	–	–	–	+0.45
SiI	+0.34	0.11	20	+0.16	0.18	8	+0.25
SiII	+0.18	–	1	–	–	–	+0.17
SI*	+0.27	0.13	2	+0.14	0.14	3	+0.26
KI*	-0.10	0.12	1	+0.10	0.12	1	-0.01
CaI	+0.05	0.14	10	-0.15	0.12	7	+0.03
ScII	+0.15	0.18	7	+0.11	0.13	3	+0.14
TiI	+0.03	0.13	7	–	–	–	+0.05
TiII	+0.04	0.06	7	+0.03	–	1	+0.02
VII	+0.02	0.07	3	+0.22	–	1	+0.20
CrI	+0.00	0.18	9	–	–	–	-0.01
CrII	+0.05	0.10	8	+0.14	0.14	3	+0.06
MnI	+0.15	0.17	6	-0.14	–	1	+0.14
FeI	+0.18	0.12	137	+0.12	0.18	55	+0.18
FeII	+0.16	0.13	30	+0.13	0.11	12	+0.18
NiI	+0.11	0.11	24	+0.20	0.19	8	+0.18
SrII*	+0.05	0.15	1	+0.00	0.15	2	+0.07
YII	-0.01	0.11	6	-0.13	–	1	+0.13
BaII*	-0.15	0.10	4	-0.34	0.13	4	-0.16
NdII	-0.20	–	1	–	–	–	+0.13

* - NLTE abundances

more peculiar than the stars in NGC 6388 and 6441. It casts a doubt on the RR Lyrae classification of KP Cyg.

RR Lyrae stars and short period type II Cepheids (CWB for short, also called BL Her stars) are known to have a helium-burning core and a hydrogen-burning shell surrounding the core. In the CN cycle, ^{12}C is converted to ^{14}N through the reaction chain, $^{12}\text{C}(p,\gamma)^{13}\text{N}(\beta^+,\nu)^{13}\text{C}(p,\gamma)^{14}\text{N}$. In addition, ^{12}C may capture an α -particle to produce ^{16}O . ^{13}C may become a source of neutrons through the $^{13}\text{C}(\alpha,n)^{16}\text{O}$ reaction. The neutrons then may be captured by nuclei of the iron peak elements to create Co and Cu, as well as many other heavier elements. Analysis of the abundances of CNO as well as light, and heavy s-process elements in these stars is the key to understanding how these processes function inside a star.

Our NLTE results for CNO clearly show that carbon and nitrogen are significantly in excess in KP Cyg, while oxygen demonstrates only a moderate overabundance. An overabundance can be also noted for sodium and aluminum. Altogether these facts testify that this star has experienced dredge-up of the materials processed in CNO, NeNa (and perhaps MgAl) cycles. Similar enhancements of C and N in some of the short period type II cepheids, i.e. CWB type stars, were recently noted by Maas, Giridhar, & Lambert (2007). In Table 5 we show the values of $\log \epsilon$ (C+N+O) and $\log \epsilon$ (C+N) for our program star and several short period ($P < 7$ days) CWB stars from Maas et al. (2007). All 7 stars are more metal-rich than the RR Lyr stars in globular clusters. The Sun is listed for comparison as well (the necessary input CNO abundances are from Table 2).

Fig. 2 shows that the C and N excesses in the short period CWB stars are very similar to that of KP Cyg. As Maas et al. have suggested the excess of C must be due to helium burning during or after the core flash. The excess of N must be due to proton capture by C. The oxygen abundances do not show the great excesses of N. This means that O was not significantly enhanced by the capture of α -particles by C. The Fig. 3 shows that the high values of $\log \epsilon$ (C+N+O) is mainly due to the excess of C and N, while the influence of O is very limited. It is clear that the enhancement of N in these stars is due to the combination of the triple-alpha reaction and proton capture rather than just the re-arrangement of the original CNO isotopes.

The evidence suggests that KP Cyg probably belongs to the CWB variables rather than to the RR Lyrae stars. Another RR Lyrae star (Wallerstein et al. 2009), UY CrB, seems to be very similar to KP Cyg because it follows the same CNO trends shown in Fig. 2 and 3, and has a long period (0.929 days, Schmidt 2002). The two carbon cepheids, V553 Cen and RT TrA, first recognized by Lloyd Evans (1983) and analysed by Wallerstein and Gonzalez (1996) and by Wallerstein, Matt and Gonzalez (2000) have been included in Table 5 as well as Figures 2 and 3. Their C and N excesses are similar to those of KP Cyg. In fact, there is

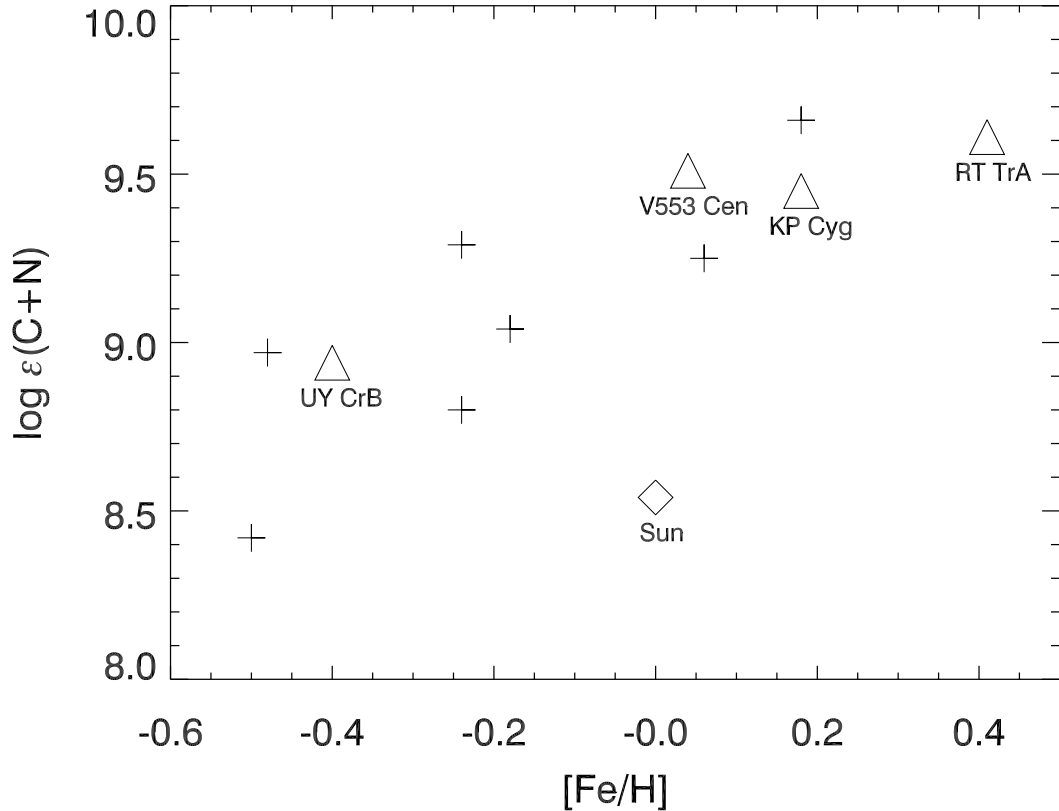


Fig. 2.—: $\log \epsilon$ (C+N) vs. $[\text{Fe}/\text{H}]$ for KP Cyg, UY CrB, the short-period CWB stars (*as plus symbols*) from Maas et al. (2007), and the Sun.

no reason why variables should be classified according to whether their periods are greater or less than the rotation period of the Earth. Once the importance of the so-called break at one day is disregarded, KP Cyg could also be a short period classical cepheid. Its low galactic latitude of 5 degrees certainly permits that.

5. Conclusion

KP Cyg has an unusually long pulsational period ($P = 0.856$ days) for an RR Lyrae star. If it is an RR Lyrae star, KP Cyg is expected to be a metal-poor star. However, the derived iron abundance completely rules out the possibility that KP Cyg is a metal-poor star. Our analysis suggests that KP Cyg is more likely a short-period CWB type star. Its

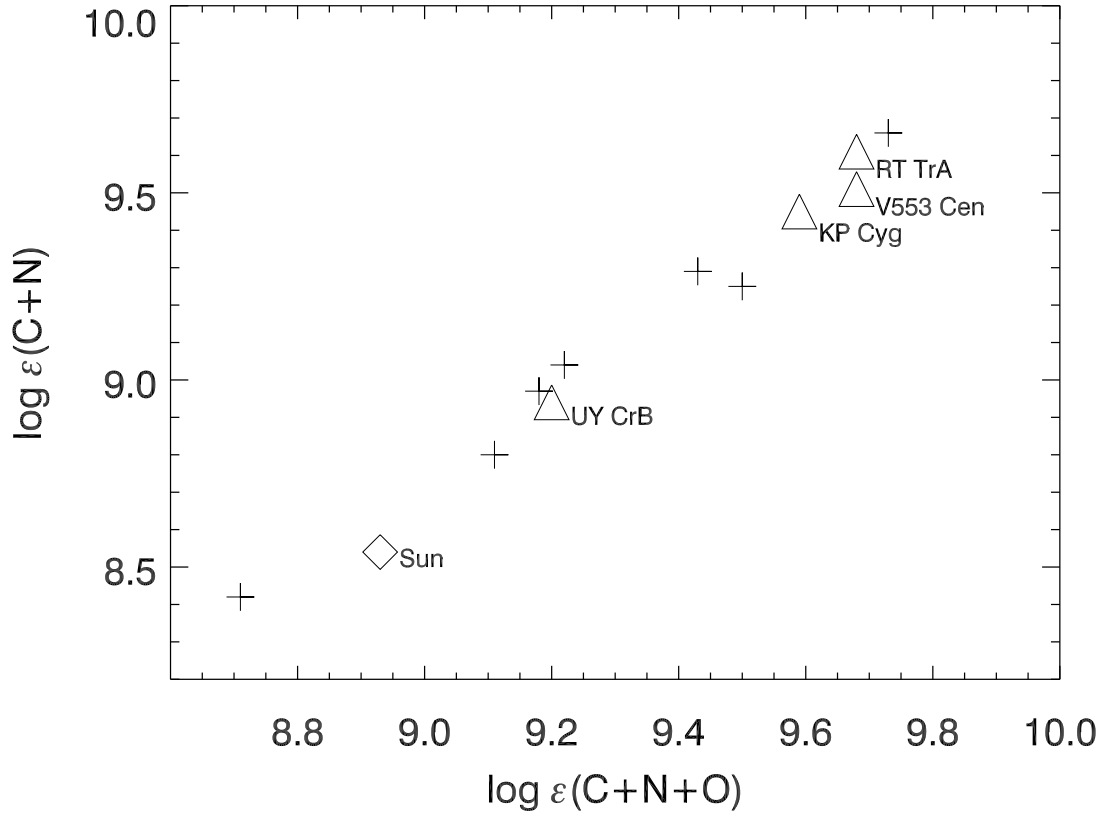


Fig. 3.—: $\log \epsilon(\text{C+N})$ vs. $\log \epsilon(\text{C+N+O})$ for KP Cyg, UY CrB, the short-period CWB stars from Maas et al. (2007)(as plus symbols), and the Sun.

low Galactic latitude of only 5 degrees is notable. The origin of the relatively metal-rich RR Lyrae and CWB stars remains uncertain since they have not been related to another population such as a globular cluster of solar metallicity. It may be necessary to reach out to dE galaxies such as the companions to M31 to find RR Lyrae or CWB type stars of solar metallicity in a system that we understand better than our own complicated Galaxy. Perhaps the 30-m telescopes now being designed will be able to accomplish that.

SMA and VVK would like to express their gratitude to the Kenilworth Fund of the New York Community Trust for the financial support of this study. The individual financial support from Kenilworth Fund was made possible through CRDF. SMA also thanks the Paris Observatory, Meudon, for its hospitality while this paper was in the final stages of

preparation. We thank Don York for the spectrum of Vesta, and Marta Mottini for reading the manuscript and making some good suggestions. We also thank the referee, George Preston, for his helpful comments. Much of the information about KP Cyg was gathered with the help of SIMBAD.

REFERENCES

- Andrievsky, S. M., Kovtyukh, V. V., Korotin, S. A., Spite, M., & Spite, F. 2001, *A&A*, 367, 605
- Andrievsky, S. M., Spite, M., Korotin, S. A., Spite, F., Bonifacio, P., Cayrel, R., Hill, V., & François P. 2007, *A&A*, 464, 1081
- Andrievsky, S. M., Spite, M., Korotin, S. A., Spite, F., Bonifacio, P., Cayrel, R., Hill, V., & François, P. 2008, *A&A*, 481, 481
- Andrievsky, S. M., Spite, M., Korotin, S. A., Spite, F., François, P., Bonifacio, P., Cayrel, R., & Hill, V. 2009, *A&A*, 494, 1083
- Andrievsky, S. M., Spite, M., Korotin, S. A., Spite, F., Bonifacio, P., Cayrel, R., François, P., & Hill, V. 2010a, *A&A*, 509, 88
- Andrievsky, S. M., Spite, M., Korotin, S. A., Spite, F., Bonifacio, P., François, P., Cayrel, R., & Hill, V. 2010b, *A&A*, submitted
- Carlsson M., 1986, *Uppsala Obs. Rep.* 33
- Clement, C. M., et al. 2001, *AJ*, 122, 2587
- Clementini, G., Carretta, E., Gratton, R., Merighi, R., Mould, J. R., & McCarthy, J. K. 1995, *AJ*, 110, 2319
- Galazutdinov, G. A. 1992, *Preprint Special Astrophysical Observatory RAS*, 92
- Gratton, R. G., Lucatello, S., Bragaglia, A., Carretta, E., Cassisi, S., Momany, Y., Pancino, E., Valenti, E., Caloi, V., Claudi, R., D’Antona, F., Desidera, S., François, P., James, G., Moehler, S., Ortolani, S., Pasquini, L., Piotto, G., & Recio-Blanco, A., 2007, *A&A*, 464, 953
- Kinemuchi, K., Smith, H. A., Wozniak, P. R., & McKay T.A. 2009, *AJ*, 132, 1202
- Korotin, S. A. 2009, *ARep*, 53, 651

- Korotin S.A., Andrievsky S.M., Luck R.E., 1999a, *A&A* 351, 168
- Korotin S.A., Andrievsky S.M., Kostynchuk L.Yu., 1999b, *Ap&SS* 260, 531
- Kovtyukh, V. V., & Andrievsky, S. M. 1999, *A&A*, 351, 597
- Kupka, F., Ryabchikova, T. A., Piskunov, N. E. et al. 2000, *Baltic Astron.*, 9,
- Kurucz, R. 1996, In *Model Atmospheres and Spectrum Synthesis*, ASPC, 108, 270
- Lloyd Evans, T. 1983, *Observatory*, 103, 276
- Loomis, Ch., Schmidt, E. G., & Simon, N. R. 1988, *MNRAS*, 235, 1059
- Lyubimkov, L. S., Lambert, D. L., Korotin, S. A., Poklad, D. B., Rachkovskaya, T. M., & Rostopchin S.I. 2010, *MNRAS*, in press
- Maas, T., Giridhar, S., & Lambert, D. L. 2007, *ApJ*, 666, 378
- Mishenina, T. V., Korotin, S. A., Klochkova, V. G., & Panchuk, V. E. 2000, *A&A*, 353, 978
- Preston, G. W. 1959, *ApJ* 130, 507
- Pritzl, B., Smith, H. A., Catelan, M., & Sweigart, A.V. 2000, *ApJ*, 530L, 41
- Schmidt, E. G. 2002, *ApJ*, 123, 965
- Smith, H. A., *RR Lyrae Stars*, 1995, Cambridge University Press
- Tsymbal, V. V. 1996, *Model Atmospheres and Spectrum Synthesis*, ed. S. J. Adelman, F. Kupka & W. W. Weiss (San Francisco), *ASP Conf. Ser.*, 108
- Vogt M., 1970, *IBVS* 468, 1
- Wallerstein, G., & Gonzalez, G. 1996, *MNRAS*, 282, 1236
- Wallerstein, G., Matt, S., & Gonzalez, G. 2000, *MNRAS*, 311, 414
- Wallerstein, G., Kovtyukh, V. V., & Andrievsky, S. M. 2009, *AJ*, 133, 1373
- Wallerstein, G., Kovtyukh, V. V., & Andrievsky, S. M. 2009, *ApJ*, 692L, 127

Table 5:: A Comparison of the combined C, N, and O abundances in KP Cyg with short-period CWB stars (Maas et al. 2007), tow carbon cepheids, and the Sun.

Star	P(days)	[Fe/H]	log $\epsilon(\text{C+N+O})$	log $\epsilon(\text{C+N})$
KP Cyg	0.9	+0.18	9.59	9.45
UY CrB	0.9	-0.40	9.20	8.94
BX Del	1.1	-0.24	9.43	9.29
VY Pyx	1.2	-0.46	9.18	8.97
BL Her	1.3	-0.18	9.22	9.04
SW Tau	1.6	+0.18	9.73	9.66
AU Peg	2.4	-0.24	9.11	8.80
DQ And	3.2	-0.50	8.71	8.42
TX Del	6.2	+0.06	9.50	9.25
V553 Cen	2.1	+0.04	9.68	9.51
RT TrA	2.0	+0.41	9.68	9.61
Sun	...	+0.00	8.93	8.54

Table A1:: Equivalent widths in the program spectra of KP Cyg

λ (Å)	Ion ^a	log gf	$\phi =$					
			0.135	0.299	0.430	0.720	0.800	0.991
			EW ^b (mÅ)					
...
6305.30	26.01	-1.80	44	0	37	0	0	0
6331.95	26.01	-1.86	43	49	49	0	0	39
6369.46	26.01	-4.14	81	94	80	72	91	0
6383.72	26.01	-2.24	44	56	55	44	63	51
...

^a Code for Ions, e.g. 26.01 = FeII

^b EW = 0 means that the EW measurement of the line is not available.